JTTEE5 18:421–426
DOI: 10.1007/s11666-009-9306-5
1059-9630/$19.00 © ASM International

Microstructure of Suspension Plasma Spray and Air Plasma Spray Al_2O_3-ZrO_2 Composite Coatings

Dianying Chen, Eric H. Jordan, and Maurice Gell

(Submitted November 22, 2008; in revised form January 8, 2009)

Al_2O_3-ZrO_2 coatings were deposited by the suspension plasma spray (SPS) molecularly mixed amorphous powder and the conventional air plasma spray (APS) Al_2O_3-ZrO_2 crystalline powder. The amorphous powder was produced by heat treatment of molecularly mixed chemical solution precursors below their crystallization temperatures. Phase composition and microstructure of the as-synthesized and heat-treated SPS and APS coatings were characterized by XRD and SEM. XRD analysis shows that the as-sprayed SPS coating is composed of α-Al_2O_3 and tetragonal ZrO_2 phases, while the as-sprayed APS coating consists of tetragonal ZrO_2, α-Al_2O_3, and γ-Al_2O_3 phases. Microstructure characterization revealed that the Al_2O_3 and ZrO_2 phase distribution in SPS coatings is much more homogeneous than that of APS coatings.

Keywords alumina, amorphous powders, plasma spray coatings, suspension plasma spray, zirconia

1. Introduction

The thermal spray process has been widely used to deposit coatings for industrial applications, including aerospace, pulp and paper, machinery, petroleum and petrochemical, biomedical, etc. (Ref 1). Thermal spray ceramic coatings are usually made from a powder feedstock. However, individual ultrafine particles (usually <5 μm) cannot be thermally sprayed using conventional powder feeder. A high carrier gas flow rate is required for the ultrafine particles penetration within the plasma jet. The high carrier gas flow rate will drastically perturb the plasma jet (Ref 2). On the other hand, these ultrafine particles would clog the hoses and fittings during transporting the powder particles from the powder feeder to the thermal spray torch (Ref 3, 4). To overcome these problems, reconstitution of individual nanoparticles into spherical micrometer-sized granules is necessary (Ref 5-7).

Recently, a suspension plasma spray (SPS) process has been developed for the deposition of various types of coatings (Ref 2, 4, 8-15). In SPS, the ultrafine or nanosized particles are dispersed in a solvent such as water or ethanol to form a suspension and then the suspension is injected into the plasma torch. The suspension droplets will undergo solvent evaporation, particles melting process in the plasma jet and form the coatings upon impacting the substrate. In both the SPS and the conventional air plasma spray (APS) processes, crystalline powders are often used. However, the preparation of crystalline powders often requires high temperature and long heat treatments. For example, Chandradass et al. (Ref 16) prepared zirconia doped alumina nanocrystalline powders at 1200 °C for 2 h. O et al. (Ref 17) synthesized α-alumina nanopowders at 1150 °C for 3 h. In contrast, preparation of amorphous powders instead of crystalline ones requires low temperature and short heat treatment, and thus decreases the powder preparation cost. So far, there is no report on the SPS nanostructured coatings using amorphous feedstock.

Alumina-zirconia composites have gained wide applications as structural ceramics or protective coatings due to their excellent mechanical and thermal properties (Ref 18-20). Al_2O_3-ZrO_2 composite exhibits higher hardness and fracture toughness and lower thermal conductivity than alumina or zirconia alone. Recently, Berghaus et al. (Ref 21) investigated the deposition of Al_2O_3-ZrO_2 composite coatings by suspension plasma spraying of submicron feedstock powders. The as-sprayed coating shows high hardness and excellent wear resistance.

In this research, Al_2O_3-ZrO_2 composite coatings were deposited by the novel SPS spraying amorphous feedstock and the conventional APS spraying Al_2O_3-ZrO_2 crystalline powder. The phase composition and microstructure of the as-sprayed and heat-treated coatings were investigated.

2. Experimental Procedures

2.1 Suspension Plasma Spray

In the SPS, molecularly mixed Al_2O_3-ZrO_2 amorphous powders were used. The Al_2O_3-ZrO_2 amorphous powders

Dianying Chen and **Maurice Gell**, Department of Chemical, Materials and Biomolecular Engineering, Institute of Materials Science, University of Connecticut, Storrs, CT 06269; **Dianying Chen**, Sulzer Metco (US) Inc., Westbury, NY 11590; and **Eric H. Jordan**, Department of Mechanical Engineering, University of Connecticut, Storrs, CT 06269. Contact e-mails: chendy@ims.uconn.edu, dianying.chen@gmail.com.

were prepared by a chemical solution process. Firstly, aluminum nitrate ($Al(NO_3)_3 \cdot 9H_2O$, powder, >97%, Alfa Aesar) and zirconium acetate ($ZrO(OOCCH_3)_2$, liquid, >99.9%, Inframat Corporation, Farmington, CT) were dissolved in deionized water based on molar volumes to produce a ceramic composition of Al_2O_3-40 wt.% ZrO_2. The obtained solution was heated at 80 °C and stirred continually to get the sol transformed into dried gel. The dried gel powders were heated to 750 °C at a heating rate of 10 °C/min, and then held for 2 h. The as-prepared powders at 750 °C are mixed in ethanol with a loading rate of 50 wt.% and then ball-milled for 24 h; ZrO_2 balls were used as ball-milling media. The phase composition and microstructure of the as-prepared and ball-milled Al_2O_3-ZrO_2 powders are shown in Fig. 1(a) and 2(a), respectively. The XRD patterns show that a large hump at ~30° is observed and no crystalline peaks appear. These results indicate that the powders are amorphous. Microstructure characterization shows the Al_2O_3-ZrO_2 powder has a size distribution of 0.2-7 μm with an average particles size of ~5 μm.

SPS is similar to the solution precursor plasma spray (SPPS); the schematic diagram can be found in previous publications (Ref 22-24). The Al_2O_3-ZrO_2 coatings were deposited using the direct current (DC) plasma torch (Metco 9MB, Sulzer Metco, Westbury, NY), which was attached to a six-axis robotic arm. Argon and hydrogen are used as the primary and the secondary plasma gases, respectively. The suspension was delivered to the atomizing nozzle by a peristaltic pump with a flow rate of 20 mL/min. Air is used as the suspension atomizing gas. The coatings were deposited on the grit-blasted (Al_2O_3 grit of #30 mesh size) 304 stainless steel disk substrates (25 mm diameter, 3 mm thickness). The surface roughness (Ra) of grit-blasted substrate is 4.68 μm measured by Zygo Profilometer (Zygo Corporation, Middlefield, CT).

2.2 Air Plasma Spray

The deposition of Al_2O_3-ZrO_2 coatings by APS is similar to the SPS process, except that the suspension

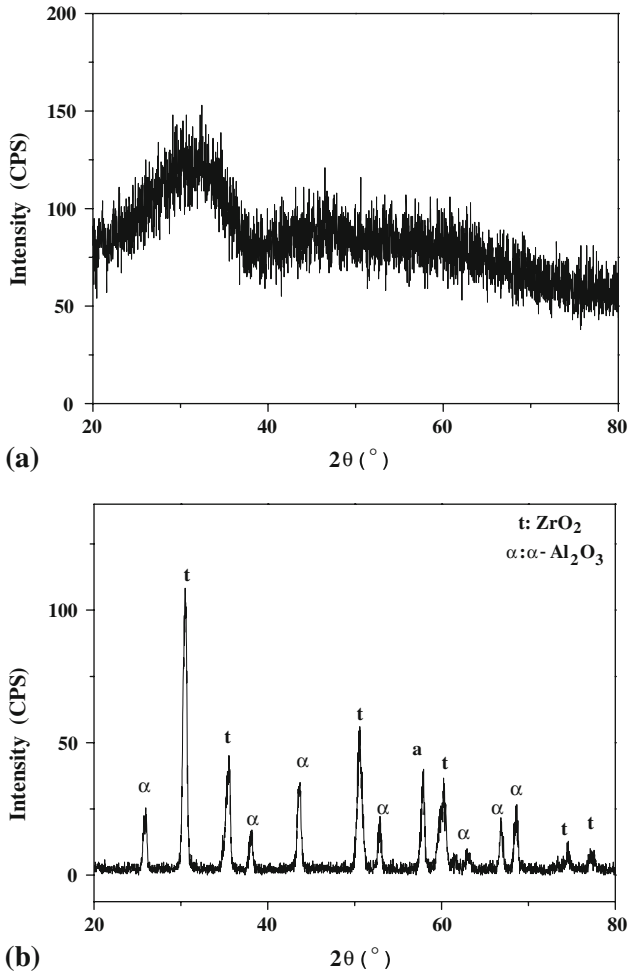

Fig. 1 XRD patterns of Al_2O_3-40 wt.% ZrO_2 feedstock powder: (a) amorphous powder for suspension plasma spray and (b) crystalline Al_2O_3-ZrO_2 powder for air plasma spray

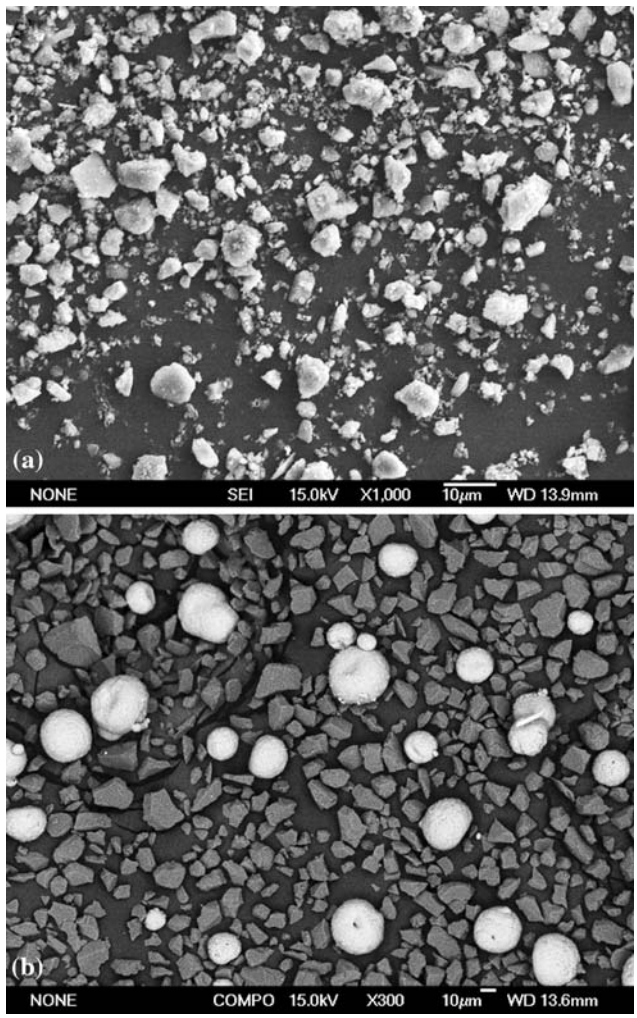

Fig. 2 SEM of Al_2O_3-40 wt.% ZrO_2 feedstock powder: (a) amorphous powder for suspension plasma spray and (b) crystalline Al_2O_3-ZrO_2 powder for air plasma spray

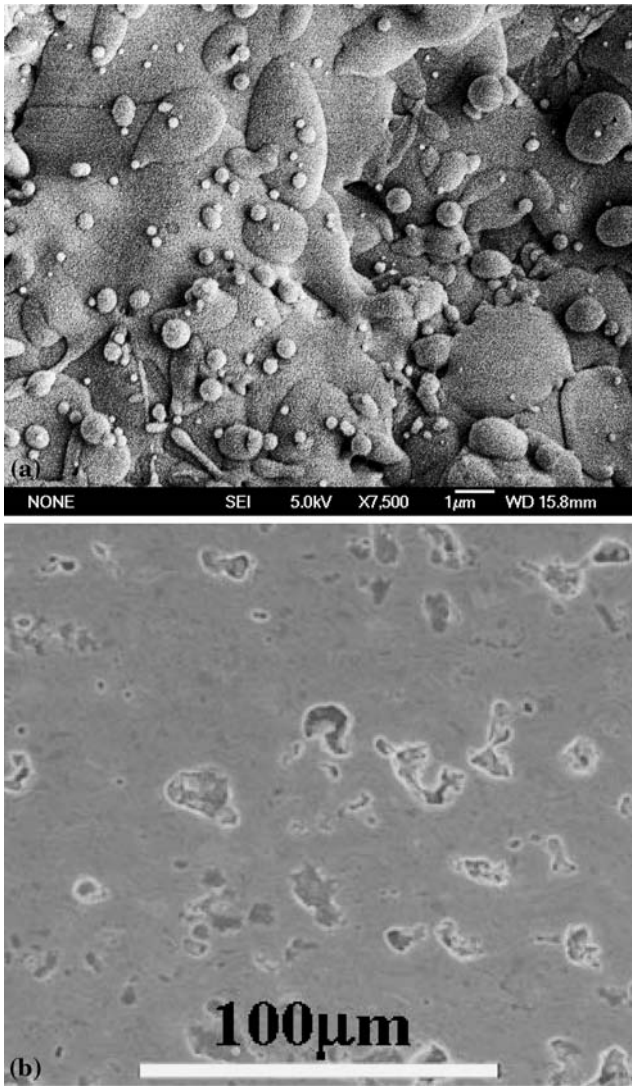

Fig. 3 Microstructure of the as-sprayed SPS coating using amorphous powder: (a) surface morphology and (b) polished cross section

Table 1 SPS and APS spray parameters

Parameters	Values	
	SPS	APS
Current, A	650	600
Voltage, V	70	65
Argon gas flow rate, SCFH	100	80
Suspension flow rate, mL/min	20	NA
Powder feeding rate, g/min	NA	27
Gun moving speed, mm/s	500	500
Spraying distance, mm	38	75
Substrate	304 stainless steel	304 stainless steel
No. of passes deposited	20	20
Coating thickness, μm	250	480
Deposition rate, μm/pass	12.5	24

feedstock is replaced by the mixed Al_2O_3-ZrO_2 commercial powders. Figures 1(b) and 2(b) show the phase composition and microstructure of the as-mixed Al_2O_3 powder (Metco 105SFP, Sulzer Metco, Westbury, NY) and ZrO_2 powder (Nanox TM S4007, Inframat Corporation, Farmington, CT) based on the composition of Al_2O_3-40 wt.% ZrO_2, respectively. The powders are composted of tetragonal zirconia and α-Al_2O_3 with particle size ranging from 10 to 60 μm. The detailed spray parameters for SPS and APS Al_2O_3-ZrO_2 coatings are summarized in Table 1.

2.3 Characterization

The crystalline phase composition of all samples was determined using x-ray diffraction (XRD, Cu Kα radiation; D5005, Bruker AXS, Karlsruhe, Germany). The XRD patterns were collected in a 2θ range from 20 to 80° with a scanning rate of 2°/min. An environmental scanning electron microscope (ESEM 2020, Philips Electron Optics, Eindhoven, The Netherlands) and a JEOL JSM-6335F field emission scanning electron microscope (FESEM, Tokyo, Japan) were used to characterize the coating microstructure. The Vickers hardness of the as-sprayed coatings was measured on the polished cross section with a 1.96 N normal load and a dwell time of 15 s. The hardness value for each sample is the average of 10 measurements.

3. Results and Discussion

3.1 As-Sprayed Coating

In the SPS process, 20 pass coating scans were carried out. Figure 3(a) shows the representative surface morphology of the as-sprayed SPS Al_2O_3-ZrO_2 coating using amorphous powder. The coating is mainly composed of ultrafine splats (1-5 μm) and dense fine spheres (~100 nm). These splats and spherical particles indicate

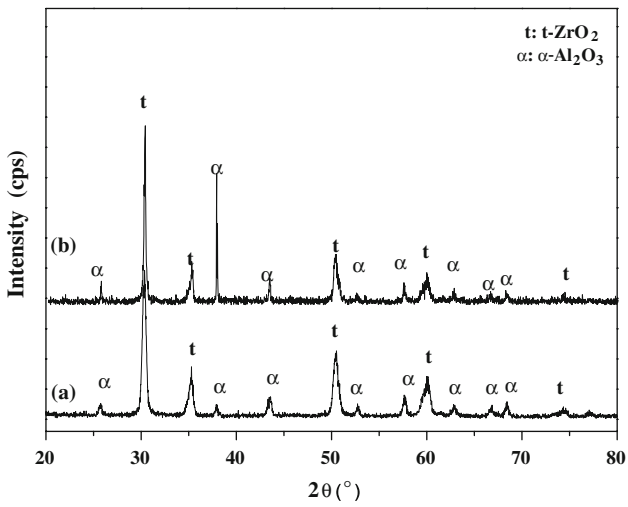

Fig. 4 XRD patterns of the SPS Al_2O_3-ZrO_2 coatings: (a) as-sprayed and (b) 1400 °C, 2 h

that the amorphous powders experience melting and solidification during coating formation. A typical polished cross section of the Al_2O_3-ZrO_2 coating is shown in Fig. 3(b). There are no coarse splat boundaries or layered structures in the as-sprayed SPS coatings. The results indicate that Al and Zr are uniformly distributed in the as-sprayed coatings. The average hardness of the as-sprayed coating is 9.9 ± 1.5 GPa. The XRD patterns (Fig. 4a) show that the as-sprayed coating is composed of α-Al_2O_3 and tetragonal ZrO_2 phases. The grain size of α-Al_2O_3 and t-ZrO_2 phases determined by the Scherrer equation is 26 and 18 nm, respectively. Thus, a nano-grained composite coating was produced.

The microstructures of the air plasma sprayed Al_2O_3-ZrO_2 coatings using crystalline Al_2O_3-ZrO_2 powder are shown in Fig. 5. Surface morphologies show that the coating is composed of large splats with diameters ranging from 50 to 100 μm. The diameter of the splats in the air plasma sprayed coating is ~30 times larger than that in the SPS coatings. Polished cross section exhibits the coating consists of multilayer structures with alternate Al_2O_3 (dark color) and ZrO_2 (bright color). For both Al_2O_3 and ZrO_2 layers, discontinuity is observed in some areas. The average hardness of the as-sprayed coating is 9.4 ± 2.0 GPa, which is very similar to that sprayed by SPS process. XRD patterns of the as-sprayed APS coatings are shown in Fig. 6(a). The coating is composed of tetragonal ZrO_2, α-Al_2O_3, and γ-Al_2O_3 phases. As is well established, γ-Al_2O_3 is one of the intermediate phases formed when alumina is melted in the plasma jet (Ref 25). Upon cooling from the melting temperature of alumina, γ-Al_2O_3 nucleates first over α-Al_2O_3; therefore, γ-Al_2O_3 typically appears in the plasma-sprayed alumina coatings. It is noted that the phase composition in the as-sprayed SPS and APS Al_2O_3-ZrO_2 coatings is a little different; there is no γ-Al_2O_3 phase observed in the as-sprayed SPS coatings though melted splats are observed (Fig. 3a). The absence of γ-Al_2O_3 phase in the SPS coating should be attributed to the process parameter effect. As seen in Table 1, the SPS coating is sprayed at 38 mm, which is within the range of plasma plume length (~50 mm); therefore, the coating surface will undergo huge convective flux from the plasma jet during deposition. The coating surface temperature measured using pyrometer is over 750 °C (Ref 26). The heat treatment from plasma jet may cause the phase transformation of intermediate γ-Al_2O_3 to stable α-Al_2O_3; therefore, only α-Al_2O_3 is observed in the as-sprayed SPS coating.

The deposition rate for SPS and APS Al_2O_3-ZrO_2 coatings is shown in Table 1. The SPS coating has a deposition rate of ~12.5 μm/pass, while the APS coating has a deposition rate of 24 μm/pass. The deposition rate for SPS coating is ~2 times less than that of APS coating.

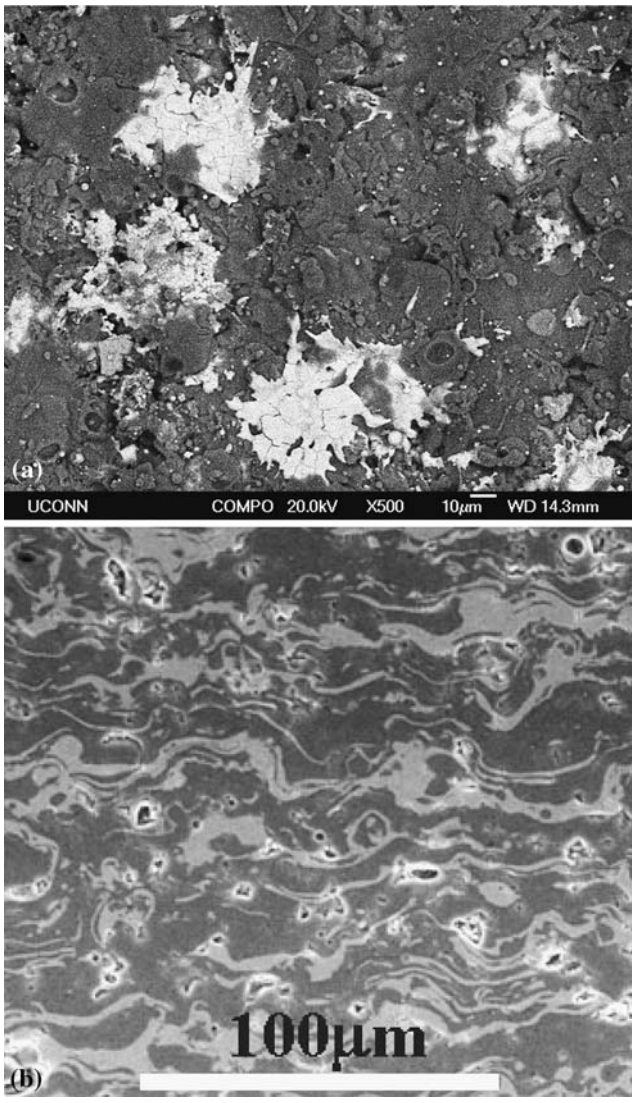

Fig. 5 Microstructure of the as-sprayed APS coating using crystalline Al_2O_3-ZrO_2 powder: (a) surface morphology and (b) polished cross section

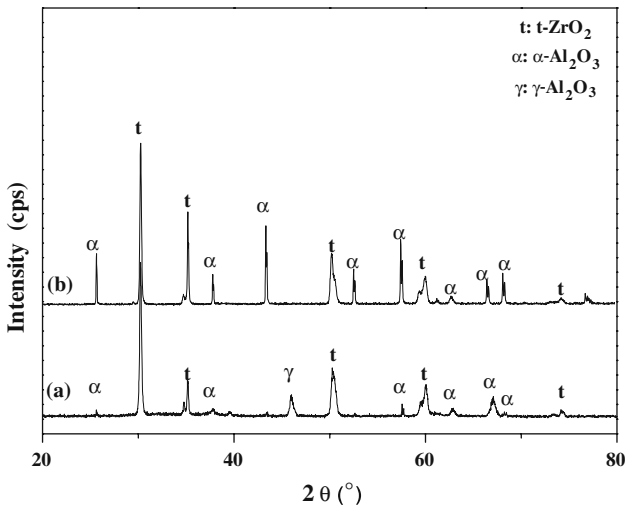

Fig. 6 XRD patterns of the APS Al_2O_3-ZrO_2 coatings: (a) as-sprayed and (b) 1400 °C, 2 h

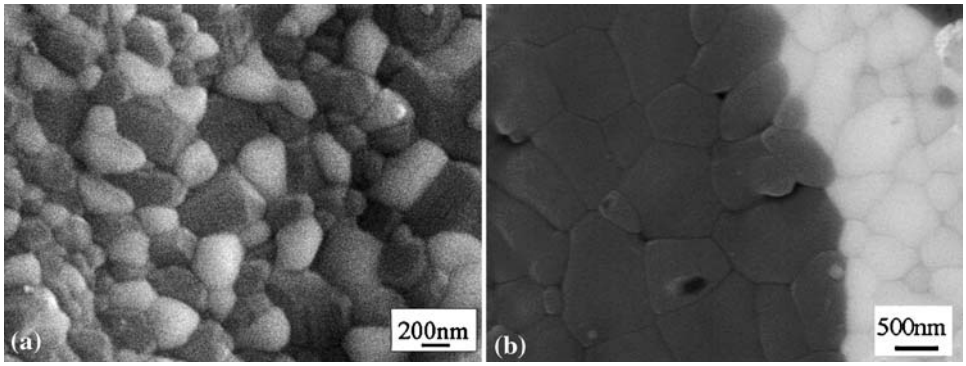

Fig. 7 Surface morphologies of the heat-treated coatings at 1400 °C for 2 h: (a) suspension plasma sprayed coating using amorphous powder and (b) air plasma sprayed coating using crystalline Al_2O_3-ZrO_2 powder

3.2 Microstructure and Phase Composition of Heat-Treated Coatings

To compare and reveal the Al_2O_3 and ZrO_2 phase distribution and microstructure in the as-sprayed SPS and APS coatings, both the as-sprayed SPS and APS coatings were heat treated at 1400 °C for 2 h. Figure 7(a) and (b) shows the heat-treated SPS and APS coating surface microstructures, respectively. It can be seen that the splats disappear and evolve to grains after heat treatment for both SPS and APS coatings. The Al_2O_3 (dark phase) and ZrO_2 (bright phase) grains in the SPS coatings are interpenetrated and distributed homogeneously. The average grains size of Al_2O_3 and ZrO_2 in the heat-treated SPS coating is about 300 and 200 nm, respectively (Fig. 7a). In contrast, Al_2O_3 (dark phase) and ZrO_2 (bright phase) grains in the heat-treated APS coatings are immiscible and a clear boundary between Al_2O_3 and ZrO_2 is observed. In addition, both Al_2O_3 and ZrO_2 grains have a faster growth rate than that in SPS coatings; the Al_2O_3 and ZrO_2 has average grain sizes of about 500 nm and 400 nm, respectively (Fig. 7b). The above results indicate that SPS process using amorphous powders as feedstock is an ideal process for the deposition of homogeneously distributed multicomponent nanostructured ceramics coatings. The homogeneously distributed phases in the composite coatings are derived from the molecularly mixed amorphous powders. The phase compositions of heat-treated SPS and APS coatings at 1400 °C for 2 h are shown in Fig. 4(b) and 6(b), respectively. Both coatings are composed of α-Al_2O_3 and tetragonal ZrO_2. γ-Al_2O_3 in the as-sprayed APS coating disappears and has transformed to stable α-Al_2O_3 after heat treatment.

4. Conclusions

Al_2O_3 and ZrO_2 composite coatings have been deposited by the suspension plasma spraying amorphous powder feedstock and the conventional APS spraying Al_2O_3-ZrO_2 crystalline powder. The coating deposition rate for SPS is ~2 times less than that of APS coating. Both the as-sprayed SPS and the APS coatings have the similar hardness with values of 9.9 ± 1.5 GPa and ~9.5 ± 2.0 GPa, respectively. The SPS coating shows much more homogeneous Al_2O_3 and ZrO_2 phase distribution than that of APS coatings. The SPS process using molecularly mixed amorphous powders as feedstock is an ideal process for the deposition of homogeneously distributed multicomponent ceramics coatings.

Acknowledgment

This work was supported by a sub-contract from Raytheon Company, from a prime contract funded by DARPA/ONR.

References

1. D. Mateyja, *Plasma Spraying of Metallic and Ceramic Coatings*, Wiley, New York, 1989
2. P. Fauchais, R. Etchart-Salas, V. Rat, J.F. Coudert, N. Caron, and K. Wittmann-Teneze, Parameters Controlling Liquid Plasma Spraying: Solutions, Sols, or Suspensions, *J. Therm. Spray Technol.*, 2008, **17**(1), p 31-59
3. R.S. Lima and B.R. Marple, Thermal Spray Coatings Engineered from Nanostructured Ceramic Agglomerated Powders for Structural, Thermal Barrier and Biomedical Applications: A Review, *J. Therm. Spray Technol.*, 2007, **16**(1), p 40-63
4. Z. Chen, R.W. Trice, M. Besser, X.Y. Yang, and D. Sordelet, Air-Plasma Spraying Colloidal Solutions of Nanosized Ceramic Powders, *J. Mater. Sci.*, 2004, **39**(13), p 4171-4178
5. M. Gell, E.H. Jordan, Y.H. Sohn, D. Goberman, L. Shaw, and T.D. Xiao, Development and Implementation of Plasma Sprayed Nanostructured Ceramic Coatings, *Surf. Coat. Technol.*, 2001, **146**, p 48-54
6. E.H. Jordan, M. Gell, Y.H. Sohn, D. Goberman, L. Shaw, S. Jiang, M. Wang, T.D. Xiao, Y. Wang, and P. Strutt, Fabrication and Evaluation of Plasma Sprayed Nanostructured Alumina-Titania Coatings with Superior Properties, *Mater. Sci. Eng. A*, 2001, **301**(1), p 80-89
7. L.L. Shaw, D. Goberman, R.M. Ren, M. Gell, S. Jiang, Y. Wang, T.D. Xiao, and P.R. Strutt, The Dependency of Microstructure and Properties of Nanostructured Coatings on Plasma Spray Conditions, *Surf. Coat. Technol.*, 2000, **130**(1), p 1-8
8. P. Fauchais, R. Etchart-Salas, C. Delbos, M. Tognonvi, V. Rat, J.F. Coudert, and T. Chartier, Suspension and Solution Plasma Spraying of Finely Structured Layers: Potential Application to SOFCs, *J. Phys. D Appl. Phys.*, 2007, **40**(8), p 2394-2406

9. I. Burlacov, J. Jirkovsky, M. Muller, and R.B. Heimann, Induction Plasma-Sprayed Photocatalytically Active Titania Coatings and Their Characterisation by Micro-Raman Spectroscopy, *Surf. Coat. Technol.*, 2006, **201**(1-2), p 255-264
10. R. Tomaszek, L. Pawlowski, L. Gengembre, J. Laureyns, Z. Znamirowski, and J. Zdanowski, Microstructural Characterization of Plasma Sprayed TiO_2 Functional Coating with Gradient of Crystal Grain Size, *Surf. Coat. Technol.*, 2006, **201**(1-2), p 45-56
11. F.L. Toma, G. Bertrand, D. Klein, C. Coddet, and C. Meunier, Nanostructured Photocatalytic Titania Coatings Formed by Suspension Plasma Spraying, *J. Therm. Spray Technol.*, 2006, **15**(4), p 587-592
12. J.O. Berghaus, B. Marple, and C. Moreau, Suspension Plasma Spraying of Nanostructured WC-12Co Coatings, *J. Therm. Spray Technol.*, 2006, **15**(4), p 676-681
13. P. Fauchais, V. Rat, U. Delbos, J.F. Coudert, T. Chartier, and L. Bianchi, Understanding of Suspension DC Plasma Spraying of Finely Structured Coatings for SOFC, *IEEE Trans. Plasma Sci.*, 2005, **33**(2), p 920-930
14. K. Wittmann-Teneze, K. Valle, L. Bianchi, R. Belleville, and N. Caron, Nanostructured Zirconia Coatings Processed by PROSOL Deposition, *Surf. Coat. Technol.*, 2008, **202**(18), p 4349-4354
15. F. Tarasi, M. Medraj, A. Dolatabadi, J. Oberste-Berghaus, and C. Moreau, Effective Parameters in Axial Injection Suspension Plasma Spray Process of Alumina-Zirconia Ceramics, *J. Therm. Spray Technol.*, 2008, **17**(5-6), p 685-691
16. J. Chandradass, J.H. Yoon, and D.S. Bae, Synthesis and Characterization of Zirconia Doped Alumina Nanopowder by Citrate-Nitrate Process, *Mater. Sci. Eng. A*, 2008, **473**(1-2), p 360-364
17. Y.T. O, S.W. Kim, and D.C. Shin, Fabrication and Synthesis of Alpha-Alumina Nanopowders by Thermal Decomposition of Ammonium Aluminum Carbonate Hydroxide (AACH), *Colloids Surf. A*, 2008, **313**, p 415-418
18. J. Chevalier, A.H. De Aza, G. Fantozzi, M. Schehl, and R. Torrecillas, Extending the Lifetime of Ceramic Orthopaedic Implants, *Adv. Mater.*, 2000, **12**(21), p 1619
19. J. Chevalier, S. Deville, G. Fantozzi, J.F. Bartolome, C. Pecharroman, J.S. Moya, L.A. Diaz, and R. Torrecillas, Nanostructured Ceramic Oxides with a Slow Crack Growth Resistance Close to Covalent Materials, *Nano Lett.*, 2005, **5**(7), p 1297-1301
20. A. Afrasiabi, M. Saremi, and A. Kobayashi, A Comparative Study on Hot Corrosion Resistance of Three Types of Thermal Barrier Coatings: YSZ, YSZ + Al_2O_3 and YSZ/Al_2O_3, *Mater. Sci. Eng. A*, 2008, **478**(1-2), p 264-269
21. J.O. Berghaus, J.G. Legoux, C. Moreau, F. Tarasi, and T. Chraska, Mechanical and Thermal Transport Properties of Suspension Thermal-Sprayed Alumina-Zirconia Composite Coatings, *J. Therm. Spray Technol.*, 2008, **17**(1), p 91-104
22. D. Chen, E.H. Jordan, and M. Gell, Effect of Solution Concentration on Splat Formation and Coating Microstructure Using the Solution Precursor Plasma Spray Process, *Surf. Coat. Technol.*, 2008, **202**(10), p 2132-2138
23. D. Chen, E.H. Jordan, M. Gell, and X. Ma, Dense Alumina-Zirconia Coatings Using the Solution Precursor Plasma Spray Process, *J. Am. Ceram. Soc.*, 2008, **91**(2), p 359-365
24. M. Gell, L.D. Xie, X.Q. Ma, E.H. Jordan, and N.P. Padture, Highly Durable Thermal Barrier Coatings Made by the Solution Precursor Plasma Spray Process, *Surf. Coat. Technol.*, 2004, **177**, p 97-102
25. R. McPherson, On the Formation of Thermally Sprayed Alumina Coatings, *J. Mater. Sci.*, 1980, **15**(12), p 3141-3149
26. D.Y. Chen, E.H. Jordan, M. Gell, and X.Q. Ma, Dense TiO_2 Coating Using the Solution Precursor Plasma Spray Process, *J. Am. Ceram. Soc.*, 2008, **91**(3), p 865-872